



# Cholinergic white matter pathways along the Alzheimer's disease continuum

Milan Nemy,<sup>1,2,3</sup> Martin Dyrba,<sup>4</sup> Frederic Brosse,<sup>5</sup> Katharina Buerger,<sup>6,7</sup> Peter Dechent,<sup>8</sup> Laura Dobisch,<sup>9</sup> Michael Ewers,<sup>6,7</sup> Klaus Fliessbach,<sup>5,10</sup> Wenzel Glanz,<sup>9</sup> Doreen Goerss,<sup>4,11</sup> Michael T. Heneka,<sup>5,10</sup> Stefan Hetzer,<sup>12</sup> Enise I. Incesoy,<sup>9,13</sup> Daniel Janowitz,<sup>7</sup> Ingo Kilimann,<sup>4,11</sup> Christoph Laske,<sup>14,15</sup> Franziska Maier,<sup>16</sup> Matthias H. Munk,<sup>14,15</sup> Robert Perneczky,<sup>6,17,18,19,20</sup> Oliver Peters,<sup>21,22</sup> Lukas Preis,<sup>22</sup> Josef Priller,<sup>21,23,24,25</sup> Boris-Stephan Rauchmann,<sup>17</sup> Sandra Röske,<sup>5</sup> Nina Roy,<sup>5</sup> Klaus Scheffler,<sup>26</sup> Anja Schneider,<sup>5,10</sup> Björn H. Schott,<sup>27,28,29</sup> Annika Spottke,<sup>5,30</sup> Eike J. Spruth,<sup>21,23</sup> Michael Wagner,<sup>5,10</sup> Jens Wiltfang,<sup>27,28,31</sup> Renat Yakupov,<sup>9</sup> Maria Eriksdotter,<sup>3,32</sup> Eric Westman,<sup>3,33</sup> Olga Stepankova,<sup>2</sup> Lenka Vyslouzilova,<sup>2</sup> Emrah Düzel,<sup>9,13</sup> Frank Jessen,<sup>5,16,34</sup> Stefan J. Teipel<sup>4,11,†</sup> and Daniel Ferreira<sup>3,†</sup>

<sup>†</sup>These authors contributed equally to this work.

Previous studies have shown that the cholinergic nucleus basalis of Meynert and its white matter projections are affected in Alzheimer's disease dementia and mild cognitive impairment. However, it is still unknown whether these alterations can be found in individuals with subjective cognitive decline, and whether they are more pronounced than changes found in conventional brain volumetric measurements. To address these questions, we investigated microstructural alterations of two major cholinergic pathways in individuals along the Alzheimer's disease continuum using an *in vivo* model of the human cholinergic system based on neuroimaging.

We included 402 participants (52 Alzheimer's disease, 66 mild cognitive impairment, 172 subjective cognitive decline and 112 healthy controls) from the Deutsches Zentrum für Neurodegenerative Erkrankungen Longitudinal Cognitive Impairment and Dementia Study. We modelled the cholinergic white matter pathways with an enhanced diffusion neuroimaging pipeline that included probabilistic fibre-tracking methods and prior anatomical knowledge. The integrity of the cholinergic white matter pathways was compared between stages of the Alzheimer's disease continuum, in the whole cohort and in a CSF amyloid-beta stratified subsample. The discriminative power of the integrity of the pathways was compared to the conventional volumetric measures of hippocampus and nucleus basalis of Meynert, using a receiver operating characteristics analysis. A multivariate model was used to investigate the role of these pathways in relation to cognitive performance.

We found that the integrity of the cholinergic white matter pathways was significantly reduced in all stages of the Alzheimer's disease continuum, including individuals with subjective cognitive decline. The differences involved posterior cholinergic white matter in the subjective cognitive decline stage and extended to anterior frontal white matter in mild cognitive impairment and Alzheimer's disease dementia stages. Both cholinergic pathways and conventional volumetric measures showed higher predictive power in the more advanced stages of the disease, i.e. mild cognitive impairment and Alzheimer's disease dementia. In contrast, the integrity of cholinergic pathways was more informative in distinguishing subjective cognitive decline from healthy controls, as compared with the volumetric measures. The multivariate model revealed a moderate contribution of the cholinergic white matter pathways but

Received June 12, 2022. Revised September 12, 2022. Accepted September 19, 2022. Advance access publication October 26, 2022

© The Author(s) 2022. Published by Oxford University Press on behalf of the Guarantors of Brain.

This is an Open Access article distributed under the terms of the Creative Commons Attribution-NonCommercial License (<https://creativecommons.org/licenses/by-nc/4.0/>), which permits non-commercial re-use, distribution, and reproduction in any medium, provided the original work is properly cited. For commercial re-use, please contact [journals.permissions@oup.com](mailto:journals.permissions@oup.com)

not of volumetric measures towards memory tests in the subjective cognitive decline and mild cognitive impairment stages.

In conclusion, we demonstrated that cholinergic white matter pathways are altered already in subjective cognitive decline individuals, preceding the more widespread alterations found in mild cognitive impairment and Alzheimer's disease. The integrity of the cholinergic pathways identified the early stages of Alzheimer's disease better than conventional volumetric measures such as hippocampal volume or volume of cholinergic nucleus basalis of Meynert.

- 1 Department of Cybernetics, Faculty of Electrical Engineering, Czech Technical University in Prague, Prague, Czech Republic
- 2 Department of Biomedical Engineering and Assistive Technology, Czech Institute of Informatics, Robotics and Cybernetics, Czech Technical University in Prague, Prague, Czech Republic
- 3 Division of Clinical Geriatrics, Center for Alzheimer Research, Department of Neurobiology, Care Sciences and Society, Karolinska Institute, Stockholm, Sweden
- 4 German Center for Neurodegenerative Diseases (DZNE), Rostock, Germany
- 5 German Center for Neurodegenerative Diseases (DZNE), Bonn, Germany
- 6 German Center for Neurodegenerative Diseases (DZNE), Munich, Germany
- 7 Institute for Stroke and Dementia Research (ISD), University Hospital, LMU Munich, Munich, Germany
- 8 MR-Research in Neurosciences, Department of Cognitive Neurology, Georg-August-University Goettingen, Goettingen, Germany
- 9 German Center for Neurodegenerative Diseases (DZNE), Magdeburg, Germany
- 10 Department for Neurodegenerative Diseases and Geriatric Psychiatry, University Hospital Bonn, Bonn, Germany
- 11 Department of Psychosomatic Medicine, Rostock University Medical Center, Rostock, Germany
- 12 Berlin Center for Advanced Neuroimaging, Charité—Universitätsmedizin Berlin, Berlin, Germany
- 13 Institute of Cognitive Neurology and Dementia Research, Otto-von-Guericke University, Magdeburg, Germany
- 14 German Center for Neurodegenerative Diseases (DZNE), Tübingen, Germany
- 15 Section for Dementia Research, Hertie Institute for Clinical Brain Research and Department of Psychiatry and Psychotherapy, University of Tübingen, Tübingen, Germany
- 16 Department of Psychiatry, Medical Faculty, University of Cologne, Cologne, Germany
- 17 Department of Psychiatry and Psychotherapy, University Hospital, LMU Munich, Munich, Germany
- 18 Munich Cluster for Systems Neurology (SyNergy), Munich, Germany
- 19 Ageing Epidemiology Research Unit (AGE), School of Public Health, Imperial College London, London, UK
- 20 Sheffield Institute for Translational Neurosciences (SITraN), University of Sheffield, Sheffield, UK
- 21 German Center for Neurodegenerative Diseases (DZNE), Berlin, Germany
- 22 Department of Psychiatry, Charité-Universitätsmedizin Berlin, Campus Benjamin Franklin, Berlin, Germany
- 23 Department of Psychiatry and Psychotherapy, Charité, Berlin, Germany
- 24 Department of Psychiatry and Psychotherapy, School of Medicine, Technical University of Munich, Munich, Germany
- 25 Centre for Clinical Brain Sciences, University of Edinburgh and UK DRI, Edinburgh, UK
- 26 Department for Biomedical Magnetic Resonance, University of Tübingen, Tübingen, Germany
- 27 German Center for Neurodegenerative Diseases (DZNE), Goettingen, Germany
- 28 Department of Psychiatry and Psychotherapy, University Medical Center Goettingen, University of Goettingen, Goettingen, Germany
- 29 Leibniz Institute for Neurobiology, Magdeburg, Germany
- 30 Department of Neurology, University of Bonn, Bonn, Germany
- 31 Neurosciences and Signaling Group, Institute of Biomedicine (iBiMED), Department of Medical Sciences, University of Aveiro, Aveiro, Portugal
- 32 Theme Inflammation and Aging, Karolinska University Hospital, Stockholm, Sweden
- 33 Department of Neuroimaging, Centre for Neuroimaging Science, Institute of Psychiatry, Psychology, and Neuroscience, King's College London, London, UK
- 34 Excellence Cluster on Cellular Stress Responses in Aging-Associated Diseases (CECAD), University of Cologne, Cologne, Germany

Correspondence to: Daniel Ferreira  
 Division of Clinical Geriatrics, Center for Alzheimer Research  
 Department of Neurobiology, Care Sciences and Society  
 NEO floor 7th, Karolinska Institutet, 141 57  
 Huddinge, Stockholm, Sweden  
 E-mail: daniel.ferreira.padilla@ki.se

**Keywords:** cholinergic system; nucleus basalis of Meynert; Alzheimer's disease; CSF markers; MRI

## Introduction

Current research in the field of Alzheimer's disease<sup>1–3</sup> suggests that pathological changes in the human brain can be observed decades before the onset of clinically detectable dementia.<sup>4</sup> Therefore, a disease continuum has been described, ranging from subjective cognitive decline (SCD) or preclinical Alzheimer's disease to mild cognitive impairment (MCI) and fully developed dementia.<sup>5</sup> In the later stages of the continuum, major pathological and clinical changes are present, e.g. extracellular amyloid-beta (A $\beta$ ) plaques and intracellular neurofibrillary tangle pathology, memory loss and other cognitive alterations.<sup>6</sup> However, the brain changes taking place in the very early stages are less known. Capturing the earliest neurodegenerative changes is challenging because conventional quantitative biomarkers might not be sensitive enough.

Neurons in the hippocampus, basal forebrain (BF) and its sub-region including the nucleus basalis of Meynert (NBM), are selectively vulnerable to Alzheimer's disease pathology.<sup>7</sup> Both hippocampus and NBM are among the first brain structures to show signs of deterioration. They can be assessed through *in vivo* volumetric measurements based on MRI.<sup>8</sup> Recent studies have shown that NBM volume is an earlier biomarker of Alzheimer's disease-like neurodegeneration, as compared with the more conventional hippocampal volumetric measures.<sup>9</sup> This finding suggests that the loss of NBM neurons might be one of the earliest events of neurodegeneration in Alzheimer's disease. The NBM and its cholinergic circuitry are heavily involved in cognitive decline characteristic of aging and age-related disorders, including Alzheimer's disease.<sup>10</sup> Furthermore, neurons with long axonal connections are particularly susceptible to Alzheimer's disease-related pathology.<sup>11</sup> These vulnerable groups of neurons seem to follow a dying-back pattern of degeneration, in which defects in myelination and synaptic dysfunction forego somatic cell death.<sup>11</sup> There is also evidence that the early white matter (WM) changes can be observed *in vivo* using diffusion MRI.<sup>12,13</sup> A recent study demonstrated alterations in mean diffusivity of NBM WM projections in patients with Alzheimer's disease and patients with MCI, using diffusion MRI.<sup>14</sup> What remains unknown is how cholinergic projections change in the preclinical stage of Alzheimer's disease and how these changes relate to other common biomarkers.

The overall goal of the current study was to investigate neurodegeneration of the human cholinergic system using diffusion-weighted MRI across the stages of the Alzheimer's disease continuum. We hypothesized that microstructural biomarkers (diffusion-based imaging indices) would detect signs of neurodegeneration earlier in the Alzheimer's disease continuum than conventional volumetric measures (hippocampal and NBM volumes). Our first aim was to investigate differences in cholinergic WM pathways between stages of the Alzheimer's disease continuum and a control group (healthy controls, HC), and to compare their predictive power to the volumetric measures. The second aim was to demonstrate the association of WM pathways and NBM volumetric changes with cognitive performance across stages of the Alzheimer's disease continuum. As cognitive measures, we focused on attention and memory as they are known to be mediated by the cholinergic circuitry.<sup>15</sup> Our diagnostic groups of SCD, MCI and Alzheimer's disease dementia are clinically in the Alzheimer's disease continuum, but, since they rely on a clinical diagnosis, it is possible that some individuals do not have an Alzheimer's pathologic change as defined currently by a positive A $\beta$  biomarker.<sup>6</sup> For this reason, to confirm our results in a biomarker-supported Alzheimer's disease continuum subsample,

we repeated all our analyses in a subsample of amyloid-positive SCD, MCI and Alzheimer's disease dementia groups, as well as amyloid-negative HC.

## Materials and methods

### Participants

We used data from the interim baseline data set of the multicentre DZNE-longitudinal Cognitive Impairment and Dementia Study (DELCODE), conducted by the German Center for Neurodegenerative Diseases (DZNE).<sup>16</sup> After excluding all cases with insufficient image quality, diffusion MRI data from 402 participants from 10 centres were included (52 AD, 66 MCI, 172 SCD and 112 HC). The participants underwent a clinical assessment of their cognitive status, including the Mini Mental State Examination (MMSE)<sup>17</sup> and an extensive neuropsychological testing battery as described previously.<sup>16</sup> Depressive symptoms were assessed with the Geriatric Depression Scale.<sup>18</sup> The DELCODE exclusion criteria are current major depressive episode, past or present major psychiatric disorders, neurological diseases other than Alzheimer's disease or MCI, or unstable medical conditions.<sup>16</sup>

Subjective cognitive decline was defined as a persistent self-perceived cognitive impairment in the absence of objective cognitive impairment, lasting at least for 6 months and being unrelated to an acute event.<sup>19</sup> The MCI patients met the core clinical criteria for MCI according to National Institute on Aging-Alzheimer's Association (NIA-AA) workgroup guidelines.<sup>20</sup> The Alzheimer's disease patients had a clinical diagnosis of probable Alzheimer's disease dementia according to the NIA-AA workgroup guidelines.<sup>21</sup> Additionally, for a subsample, we requested amyloid positivity for the SCD, MCI and Alzheimer's disease dementia groups.

The HC participants had no objective cognitive impairment in cognitive tests, no history of neurological or psychiatric disease, and did not report a self-perceived cognitive decline. For a subsample, we requested amyloid negativity for the HC group.

All participants or their legal representatives provided written informed consent. The study protocol was approved by the local institutional review boards and ethics committees of the participating centres. DELCODE was conducted in accord with the Helsinki Declaration of 1975.

### Cognitive assessment

DELCODE uses an extensive neuropsychological test battery covering specific domains of memory, executive functions, language, visuospatial abilities, as well as attention and working memory.<sup>16</sup> The following tests of memory and attention were selected according to the aims of the current study: selected tasks of the Alzheimer's Disease Assessment Scale–Cognitive 13-item subscale (ADAS-Cog 13),<sup>22</sup> including ADAS word list learning (immediate recall), ADAS word list recall (delayed recall) and ADAS figure learning, to assess verbal and spatial episodic memory. Attention was measured with the oral form of the Symbol Digit Modalities Test<sup>23</sup> and the Trail Making Test A and B<sup>24</sup> forms.

### CSF biomarkers

Procedures for CSF acquisition, processing and analysis in DELCODE have been previously described.<sup>16</sup> In the current study, we used the CSF A $\beta$ 42/A $\beta$ 40 ratio as a biomarker for amyloid- $\beta$  pathology, CSF-phosphorylated tau181 levels as a biomarker for tau neurofibrillary tangles and total CSF tau levels as a biomarker for



unspecific neurodegeneration, according to the most recent NIA-AA guidelines AT(N) system.<sup>6</sup> The cut-off value for the A $\beta$ 42/A $\beta$ 40 ratio was <0.09, based on a previous study<sup>25</sup>: cases below the cut-off of 0.09 were designated amyloid positive and cases above the cut-off as amyloid negative. CSF biomarkers were determined using commercially available kits according to vendor specifications: V-PLEX A $\beta$  Peptide Panel 1 (6E10) Kit (K15200E) and V-PLEX Human Total Tau Kit (K151LAE) (Mesoscale Diagnostics LLC), and Innostest Phospho-Tau(181P) (81 581; Fujirebio Germany GmbH).

CSF was sampled in those participants who consented to a lumbar puncture (overall CSF sampling rate in DELCODE is around 50%). In the current study, we report the data for all participants with available CSF samples ( $n=185$ ; [Supplementary Table 1](#)). Participants with CSF samples did not differ from participants without CSF samples ( $n=217$ ) in key demographic variables and MMSE scores ([Supplementary Table 2](#)).

### APOE genotyping

Genotypes for rs7412 and rs429358, the single nucleotide polymorphisms (SNPs) defining the  $\epsilon$ -2,  $\epsilon$ -3 and  $\epsilon$ -4 alleles of APOE, were genotyped using the commercially available TaqMan<sup>®</sup> SNP Genotyping Assay (ThermoFisher Scientific). Both SNP assays were amplified on genomic DNA using a StepOnePlus Real-Time Polymerase Chain Reaction System (ThermoFisher Scientific). Visual inspection of cluster formation was performed for each SNP before genotype data were used to define  $\epsilon$ -2,  $\epsilon$ -3 and  $\epsilon$ -4 alleles in each sample. Participants were classified as APOE4 carriers if they were  $\epsilon$ 3/ $\epsilon$ 4 or  $\epsilon$ 4/ $\epsilon$ 4 carriers.

### MRI acquisition

The data were acquired from ten Siemens 3.0 T MRI scanners using identical acquisition parameters and harmonized procedures. To ensure high image quality throughout the acquisition phase, all scans had to pass a semiautomated quality check during the study conduction so that protocol deviations could be reported to the study sites, and the acquisition at the respective site could be adjusted.

High-resolution T<sub>1</sub>-weighted anatomical images were obtained using a sagittal magnetization-prepared rapid gradient echo sequence (field of view 256×256 mm, matrix size 256×256, isotropic voxel size 1 mm, echo time 4.37 ms, flip angle 7°, repetition time 2500 ms, number of slices 192, parallel imaging acceleration factor 2).

An axial diffusion sequence was measured on the basis of a single-shot echo-planar imaging (EPI) multi-shell sequence (field of view 240×240 mm, matrix size 120×120, isotropic voxel size 2 mm, repetition time 12 100 ms, echo time 88 ms, flip angle 90°, number of slices 72, parallel imaging acceleration factor 2) with two diffusion-weighted shells at  $b=700$  s/mm<sup>2</sup> (30 volumes) and  $b=1000$  s/mm<sup>2</sup> (30 volumes). The sequence included 10 non-diffusion-weighted scans ( $b=0$  s/mm<sup>2</sup>) evenly interspersed throughout the diffusion-weighted volumes.

A B0 field map was collected with matching geometry for use in unwarping EPI distortions due to magnetic field inhomogeneity.<sup>26</sup> The field map acquisition was performed with a 3D dual-echo spoiled gradient echo pulse sequence (field of view 240×240 mm, matrix size 80×80, isotropic voxel size 3 mm, number of slices 48, repetition time 675 ms, echo time 1=4.92 ms, echo time 2=7.38 ms, flip angle 60°).

### Diffusion MRI-based modelling of the human cholinergic system

To characterize the microstructural properties of the human cholinergic system, a diffusion MRI-based *in vivo* model was derived. We followed the procedure described in a previous study.<sup>27</sup> Briefly, the diffusion-weighted imaging data were preprocessed using FSL (FMRIB Software Library).<sup>28</sup> The non-brain tissue was removed,<sup>29</sup> EPI distortion was corrected using EPI-based field mapping<sup>30</sup> and eddy currents and head motion were corrected.<sup>31</sup>

The estimation of the diffusion parameters in a standard ball-and-sticks model<sup>32</sup> for each voxel was performed with the graphics processing units accelerated version of the bedpostX toolbox,<sup>33</sup> considering three fibres modelled per voxel.

Next, two WM pathways originating from the NBM were captured, one traversing through the cingulum and one through the external capsule.<sup>34</sup> The NBM region of interest (ROI) was based on a cytoarchitectonic map of BF cholinergic nuclei in MNI space, derived from combined histology and *in cranio* MRI of a post-mortem brain.<sup>35</sup> The cingulum and external capsule masks were based on the Johns Hopkins University (JHU) WM atlas, available as part of the FSL package.<sup>36</sup>

Probabilistic tracking was performed by repeating 5000 random samples from each of the NBM ROI voxels and propagated through the local probability density functions of the estimated diffusion parameters.<sup>37</sup> Only the tracts traversing through the cingulum or external capsule ROI were kept.

Next, an unbiased template was created based on B0 preprocessed images from all HC cases using the Advanced Normalization Tools (<http://stnava.github.io/ANTs/>). After that, both pathways (through cingulum and external capsule) of all HC cases were non-linearly warped into the space of this unbiased template. Finally, pathway-specific binary masks were created by considering all the individual warped tracts and retaining only the voxels that were present (i.e. met by at least one fibre) in at least 60% of the cases. The 60% group threshold was chosen by visual inspection so that the resulting pathways were extensive yet still specific.

### Extraction of diffusion indices

To characterize the microstructure properties of the tracked cholinergic pathways, we extracted the widely used indices of mean diffusivity (MD) and fractional anisotropy (FA) from the diffusion tensor model.

We calculated an average value of MD and FA indices for each participant and pathway, i.e. an average value of the diffusion index map within the cingulum and external capsule binary masks.

As a control, the remaining WM mask was created by excluding the two cholinergic WM pathways described before (i.e. a union of external capsule and cingulum pathways) from the whole WM mask. Then, we extracted the average values of MD and FA indices within the remaining WM mask using the same procedure.

We favoured the MD index to the FA index for its reduced susceptibility to the crossing-fibre problem. Nonetheless, we report FA results in the global analysis for reference.

### NBM and hippocampal volumes

To evaluate the cell body damage of the cholinergic neurons, the NBM volume was estimated from the T<sub>1</sub>-weighted MR images. First, all the images were skull-stripped<sup>29</sup> and corrected for bias field.<sup>38</sup> Then, a non-linear spatial transformation to the MNI space

where the NBM ROI resides was derived using Advanced Normalization Tools. Finally, an individual NBM volume was calculated as the number of grey matter (GM) voxels with the back-transformed NBM ROI in native T1-weighted space. The GM segmentation was obtained from the FSL's Automated Segmentation Tool.<sup>38</sup> The final NBM volume was adjusted by partial volume information provided by FSL's Automated Segmentation Tool. The total intracranial volume (TIV) was estimated based on the affine transformation in the FreeSurfer v.6.0 image analysis suite (<http://surfer.nmr.mgh.harvard.edu/>). FreeSurfer was also used to segment the hippocampus (bilateral). Both the NBM and hippocampal volumes were normalized by the TIV to account for between-subject variability in head size.<sup>39</sup>

## WM hypointensities

Previous studies have shown that the amount of small vessel disease influences the integrity of the cholinergic WM pathways.<sup>27,40</sup> Hence, we included information about small vessel disease status by means of WM hypointensities. WM hypointensities on T<sub>1</sub>-weighted images strongly correlate with WM hyperintensities as seen on T<sub>2</sub>/FLAIR images,<sup>41</sup> and with microstructural WM changes as measured on diffusion tensor imaging (DTI) data.<sup>42</sup> Segmentation of WM hypointensities and corresponding volumetrics was performed on T<sub>1</sub>-weighted images using the probabilistic procedure implemented in FreeSurfer v.6.0.<sup>43</sup>

## Statistical analysis

Statistical analysis was carried out using the R programming language (The R Foundation for Statistical Computing, v.4.0.3). Results were deemed statistically significant at two-tailed  $P < 0.05$ .

## Demographics

Demographics were group-wise compared between HC and all other diagnostic groups using independent t-tests for age and years of education, and chi-square tests for sex and APOE genotype. Differences in cognitive measures and CSF biomarkers between diagnostic groups were compared using a one-way analysis of variance with covariates (ANCOVA) with age and sex as covariates. ANCOVA was followed by paired *post hoc* t-tests adjusting for multiple comparisons with the Tukey method. Our comparisons of interest were SCD versus HC, MCI versus HC and Alzheimer's disease dementia versus HC. The extracted NBM and hippocampus volumes corrected for the TIV, and WM hypointensities load were also compared using ANCOVA, controlling for age and sex.

## Pathway integrity comparison (global and voxel-wise)

To assess the differences in the integrity of the tracked pathways between groups, we ran analysis both in aggregated (average, as a global measure) and voxel-wise manner. First, we analysed group-wise differences of the FA and MD averages in the cingulum, external capsule and remaining WM control mask using analyses of covariance (ANCOVA) with age and sex as covariates. ANCOVA was followed by paired *post hoc* t-tests adjusting for multiple comparisons with the Tukey method. Our comparisons of interest were SCD versus HC, MCI versus HC and Alzheimer's disease dementia versus HC. However, we also report the results for the remaining pairs for the sake of completeness (SCD versus MCI, SCD versus Alzheimer's disease dementia and MCI versus Alzheimer's disease dementia). Next, to assess the more detailed spatial differences in the integrity of the pathways, we applied a voxel-wise generalized

linear model using permutation-based non-parametric testing ('randomise')<sup>44</sup> and correcting for multiple comparisons across space (threshold-free cluster enhancement, TFCE), with age and sex as covariates. For this, we previously warped all individual MD maps into a common space of the unbiased template using non-linear warp field originated from registering respective individual B0 images to the unbiased template. Significance maps were corrected for multiple comparisons using a familywise error rate of  $P < 0.05$ . To assess the association between CSF biomarkers of Alzheimer's disease-related pathology and integrity in cholinergic WM pathways, we performed Pearson correlations.

## Importance analysis using random forest

To assess the association of MRI markers of the cholinergic system with cognitive performance, we conducted several random forest (RF) analyses with cognitive performance as outcome variables and MD in the cingulum WM pathway, MD in the external capsule WM pathway and NBM volume as predictors. We also included MD in the remaining WM as a negative control for the cholinergic WM. Further, we included WM hypointensities as an extra predictor because our clinical groups differed in WM-hypointensity load, and we had previously demonstrated that WM hypointensities make a major contribution to integrity in cholinergic WM pathways.<sup>27,45</sup> Finally, we also included age, sex and years of education to consider the contribution of these variables, as they usually influence cognitive performance. To compare the role of the integrity of the cholinergic pathways and the NBM volume along the Alzheimer's disease continuum, we created two separate RF models: one for HC and SCD combined, and one for MCI and Alzheimer's disease combined. We combined the groups to gain sufficient statistical power, keeping separated RF models for groups with normal cognition (HC and SCD) and groups with impaired cognition (MCI and Alzheimer's disease dementia).

We used RF regression with a conditional inference tree for unbiased variable selection. RF is an ensemble method in machine learning that involves growing multiple decision trees via bootstrap aggregation (bagging). Each tree predicts a classification independently and votes for the corresponding class. The majority of the votes decides the overall prediction.<sup>46,47</sup> RF has important advantages over other regression techniques in terms of ability to handle highly non-linear biological data, robustness to noise and tuning simplicity.<sup>48</sup>

Conditional feature importance scores for RF were computed by measuring the increase in prediction error if the values of a variable under question were permuted within a grid defined by the covariates that were associated with the variable of interest. This score was computed for each constituent tree and averaged across the entire ensemble. The conditional feature importance scores were designed to diminish an undesirable effect of preference of correlated predictor variables. Variables receiving higher importance scores are more likely to be closely linked to the output variable (cognitive scores). The RF was composed of 2000 conditional inference trees. The party package<sup>49</sup> was used for this analysis.

## Biomarker discriminative power (receiver operating characteristic analysis)

To investigate the capacity of the suggested biomarkers (integrity of all considered pathways and BF and hippocampus volumes) to discriminate the different clinical groups from the HC group, the receiver operating characteristic (ROC) curve analysis was carried out. The analysis was performed each time between the HC group and one of the clinical groups, resulting in three different performance

models (one for SCD, one for MCI and one for Alzheimer's disease dementia subjects). Next, we computed the area under the ROC curve (AUC) for each curve as a cumulative statistic of the overall discriminative power of the biomarker in question. AUCs were then pair-wise compared using the bootstrap method (2000 replications) from the 'pROC' package.<sup>50</sup>

## Data availability

Requests for access to the data and code used in this study should be directed to the corresponding author. Our data sharing complies with the requirements of our funders and institutes, as well as with institutional ethics approval. The data, which support this study, are not publically available, but may be provided upon reasonable request via <https://www.dzne.de/en/research/studies/clinical-studies/delcode>.

## Results

### Demographic characteristics, cognitive performance and MRI and CSF biomarkers across study groups

Demographic data are shown in Table 1. All clinical groups (SCD, MCI, Alzheimer's disease dementia) were significantly older than the HC group ( $P_{\text{SCD}} = 0.005$ ,  $P_{\text{MCI}} < 0.001$ ,  $P_{\text{AD}} < 0.001$ ). The SCD and MCI groups had a higher frequency of men than the HC group ( $P_{\text{SCD}} = 0.033$ ,  $P_{\text{MCI}} = 0.004$ ). The Alzheimer's disease dementia group had significantly fewer years of education ( $P_{\text{AD}} < 0.001$ ) and together with the MCI group showed worse performance in the MMSE than the HC group ( $P_{\text{MCI}} < 0.001$ ,  $P_{\text{AD}} < 0.001$ ). MCI and Alzheimer's disease dementia groups (but not SCD) performed worse than the HC group in ADAS word list learning (immediate recall) ( $P_{\text{MCI}} < 0.001$ ,  $P_{\text{AD}} < 0.001$ ), ADAS figure learning (recall) ( $P_{\text{MCI}} < 0.001$ ,  $P_{\text{AD}} < 0.001$ ), Trail making test A ( $P_{\text{MCI}} = 0.043$ ,  $P_{\text{AD}} < 0.001$ ), Trail making test B ( $P_{\text{MCI}} < 0.001$ ,  $P_{\text{AD}} < 0.001$ ) and symbol digit modalities ( $P_{\text{MCI}} < 0.001$ ,  $P_{\text{AD}} < 0.001$ ). There were differences in ADAS word list learning (delayed recall) in all diagnostic groups when compared with the HC group ( $P_{\text{SCD}} = 0.043$ ,  $P_{\text{MCI}} < 0.001$ ,  $P_{\text{AD}} < 0.001$ ).

NBM and hippocampal volumes were significantly lower in all clinical groups as compared with the HC group (NBM volume:  $P_{\text{SCD}} = 0.049$ ,  $P_{\text{MCI}} < 0.001$ ,  $P_{\text{AD}} < 0.001$ , hippocampal volume:  $P_{\text{SCD}} = 0.018$ ,  $P_{\text{MCI}} < 0.001$ ,  $P_{\text{AD}} < 0.001$ ), with age and sex adjusted in the model. WM-hypointensity volume was significantly higher only in MCI and Alzheimer's disease dementia groups as compared with the HC group ( $P_{\text{MCI}} = 0.031$ ,  $P_{\text{AD}} < 0.001$ ), with age and sex adjusted in the model. The frequency of APOE4 carriers was significantly higher only in the MCI and AD groups in comparison to the HC group ( $P_{\text{MCI}} < 0.001$ ,  $P_{\text{AD}} < 0.001$ ). Qualitative inspection shows that 31% of the SCD individuals were APOE4 carriers, while only 22% of the HC individuals were APOE4 carriers.

The subset with available CSF biomarkers ( $n = 185$ , 46% of the total sample) showed no significant differences between SCD and HC groups in any of the CSF biomarkers. On the other hand, MCI and Alzheimer's disease dementia groups showed a significant decrease in the  $A\beta_{42}/A\beta_{40}$  ratio, and a significant increase in total tau and p-tau181 levels ( $A\beta_{42}/A\beta_{40}$  ratio:  $P_{\text{MCI}} < 0.001$ ,  $P_{\text{AD}} < 0.001$ , total tau:  $P_{\text{MCI}} = 0.035$ ,  $P_{\text{AD}} < 0.001$ , p-tau181:  $P_{\text{MCI}} = 0.044$ ,  $P_{\text{AD}} < 0.001$ ), as compared with the HC group. Moreover, MCI and Alzheimer's disease dementia groups also showed a significant decrease in the  $A\beta_{42}/A\beta_{40}$  ratio, and a significant increase in total tau and p-tau181 levels ( $P < 0.001$  in all comparisons), as compared with the SCD group. All CSF biomarker analyses included age and sex as covariates.

### Integrity of cholinergic pathways along the AD continuum: global analysis

Figure 1 and Supplementary Table 6 show the average FA and MD values of the tracked pathways along the Alzheimer's disease continuum, with all analyses controlled for age and sex. We observed a significant average decrease of FA and an average increase of MD in SCD individuals as compared with the HC group ( $P < 0.001$  in all comparisons, for both pathways), demonstrating early alterations of cholinergic pathways in the Alzheimer's disease continuum.

The same differences in FA and MD average measures were observed in the MCI and Alzheimer's disease dementia groups compared to the HC group ( $P < 0.001$  in all comparisons, for both pathways). In the remaining WM, only the average FA values in MCI and Alzheimer's disease, and the average MD values in SCD and Alzheimer's disease showed significant differences when compared to the HC group (average FA:  $P_{\text{MCI}} = 0.002$ ,  $P_{\text{AD}} < 0.001$ , average MD:  $P_{\text{SCD}} = 0.020$ ,  $P_{\text{AD}} < 0.001$ ).

In the amyloid stratified subsample, we observed a similar pattern of findings in both cholinergic pathways (Supplementary Fig. 1). In contrast with the whole sample, the group differences in the remaining WM in SCD and MCI groups when compared to the HC group were non-significant.

All pair-wise post hoc statistics are summarized in Supplementary Tables 3 and 4.

Last, we observed a statistically significant correlation between integrity of cholinergic WM pathways with CSF biomarkers of Alzheimer's disease pathology: MD in cingulum pathway and  $A\beta_{42/40}$ :  $r_{(183)} = -0.221$ ,  $P < 0.01$ ; MD in external capsule pathway and  $A\beta_{42/40}$ :  $r_{(183)} = -0.248$ ,  $P < 0.001$ ; MD in cingulum pathway and p-tau:  $r_{(183)} = 0.169$ ,  $P < 0.05$ ; MD in external capsule pathway and p-tau:  $r_{(183)} = 0.199$ ,  $P < 0.01$ ; MD in cingulum pathway and total tau:  $r_{(183)} = 0.198$ ,  $P < 0.01$ ; and MD in external capsule pathway and total tau:  $r_{(183)} = 0.247$ ,  $P < 0.001$ .

### Integrity of cholinergic pathways along the Alzheimer's disease continuum: regional (voxel-wise) analysis

Figures 2 and 3 show statistical maps of voxel-wise differences in MD between groups, in cingulum and external capsule pathways. All analyses were controlled for age and sex.

The cingulum pathway (Fig. 2) showed significantly higher MD values in the retrosplenial and posterior cingulate already in the SCD group when compared with the HC, suggesting an early regional vulnerability of posterior cholinergic WM in the Alzheimer's disease continuum.

In the MCI group, these differences were spatially more pronounced and complemented by significant differences in a small area in the rostral anterior cingulate. In the Alzheimer's disease dementia group, all the differences visible in the MCI group were present, but further spatially extended and were statistically more pronounced with additional significant differences in the dorsal anterior cingulate. Differences in MD values in the WM underneath NBM emerged only in the MCI and Alzheimer's disease dementia groups, but not in the SCD group, when compared with the HC group. This could suggest that it is distal cholinergic WM what shows the earliest alterations in the Alzheimer's disease continuum.

The external capsule pathway (Fig. 3) showed a resembling pattern of differences in MD values in the SCD and MCI groups: in the external capsule, retrosplenial and posterior cingulate, and parts of



Table 1 Demographic and clinical variables by group

	Whole sample	HC	SCD	MCI	AD dementia	F-value/ $\chi^2$ -value
n	402	112	172	66	52	
Age	71.5 (6.5) [59–89]	69.1 (5.6) [60–81]	71.6 (6.3)** [59–87]	72.6 (6.4)** [61–86]	75.2 (6.8)*** [60–89]	12.6, $P < 0.001$
Sex (M/F)	210/192	48/64	96/76*	43/23**	23/29 <sup>ns</sup>	10.6, $P < 0.05$
Years of education	14.3 (3.0)	14.8 (2.7)	14.5 (3.0) <sup>ns</sup>	14.1 (3.1) <sup>ns</sup>	12.6 (3.0)***	6.9, $P < 0.001$
MMSE total score	28.1 (2.9)	29.4 (0.9)	29.2 (0.9) <sup>ns</sup>	27.8 (1.8)***	21.9 (3.1)***	324, $P < 0.001$
ADAS word list learning (immediate recall)	19.8 (5.5)	23.2 (3.5)	21.6 (3.7) <sup>ns</sup>	16.4 (3.9)***	10.7 (4.0)***	151, $P < 0.001$
ADAS word list recall (delayed recall)	6.20 (2.95)	8.09 (1.62)	7.23 (1.78)*	4.03 (2.44)***	1.24 (1.61)***	191, $P < 0.001$
ADAS figure learning (recall)	8.35 (3.40)	9.99 (1.60)	9.78 (1.79) <sup>ns</sup>	6.64 (3.22)***	1.98 (2.18)***	201, $P < 0.001$
Trail making test A	51.0 (30.3)	43.9 (17.3)	41.0 (14.7) <sup>ns</sup>	57.0 (27.1)*	94.2 (52.2)***	52.0, $P < 0.001$
Trail making test B	116.6 (62.8)	90.5 (25.8)	101.0 (38.4) <sup>ns</sup>	133.0 (60.7)***	244.0 (84.0)***	100, $P < 0.001$
Symbol digit modalities test	42.4 (13.3)	49.6 (9.2)	45.7 (9.8) <sup>ns</sup>	37.3 (9.8)***	21.2 (12.0)***	90.0, $P < 0.001$
NBM volume ( $\mu$ l) (TIV corrected)	236 (68)	272 (50)	246 (61)*	208 (62)***	160 (58)***	39.1, $P < 0.001$
hippocampal volume ( $\mu$ l) (TIV corrected)	6000 (1100)	6680 (870)	6200 (1100)*	5430 (950)***	4790 (870)***	43.9, $P < 0.001$
WMH load ( $\mu$ l)	3954 (4826)	2421 (3311)	3516 (3870) <sup>ns</sup>	5071 (5654)*	7285 (7039)***	9.7, $P < 0.001$
APOE genotype, n	388	109	166	63	50	
APOE4 genotype, n (%)	132 (34.0)	24 (22.0)	51 (30.7) <sup>ns</sup>	30 (47.6)***	27 (54.0)***	21.9, $P < 0.001$
CSF biomarkers, n	185	40	73	47	25	
A $\beta$ <sub>42</sub> /A $\beta$ <sub>40</sub>	0.079 (0.029)	0.097 (0.023)	0.088 (0.027) <sup>ns</sup>	0.066 (0.028)***	0.052 (0.017)***	17.3, $P < 0.001$
total tau (pg/ml)	486 (299)	368 (143)	378 (188) <sup>ns</sup>	544 (257)*	883 (438)***	23.1, $P < 0.001$
p-tau181 (pg/ml)	64.1 (36.7)	51.3 (17.3)	52.5 (24.7) <sup>ns</sup>	70.1 (31.8)*	107.0 (58.4)***	16.8, $P < 0.001$

Variables in the SCD, MCI and AD dementia groups were all statistically compared to the corresponding variable in the HC group. For age and years of education an independent t-test was performed. For sex and APOE4 genotype, a chi-square test was performed. For all other variables, one-way ANCOVA were performed by setting a diagnostic group as the independent variable and age and sex as covariates. P-values result from post hoc tests between a diagnostic group and HC with Tukey correction for multiple comparisons. ns, not statistically significant ( $P > 0.05$ ), \* $P < 0.05$ , \*\* $P < 0.01$ , \*\*\* $P < 0.001$  (assessed using a two-tailed alpha). Values reflect mean value (SD) [range] or count. AD = Alzheimer’s disease; M = male; F = female; WMH = WM hypointensities.

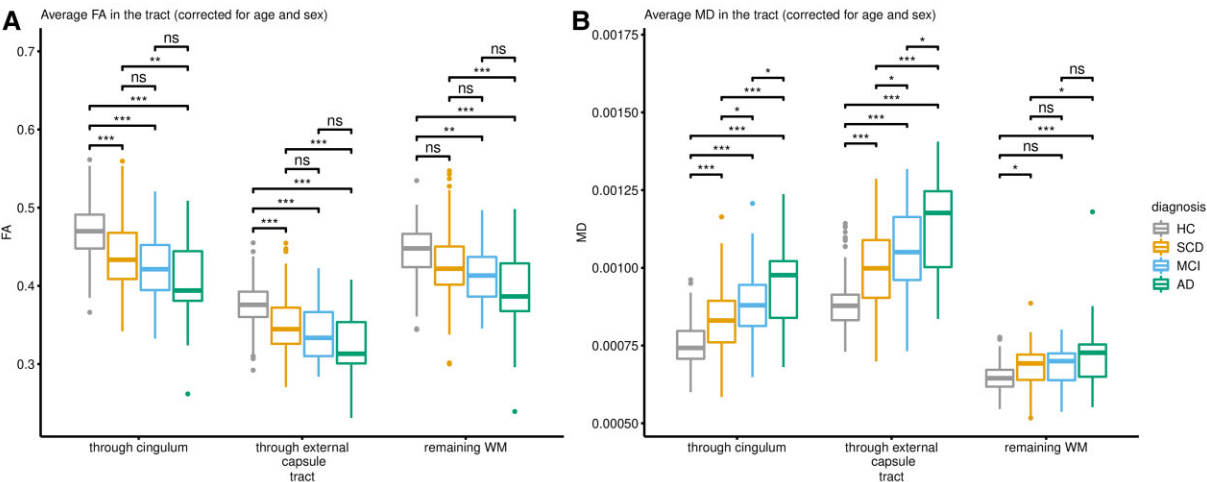


Figure 1 Parameters of diffusivity in cholinergic pathways and remaining WM. All clinical groups differed in FA and MD compared to the HC groups in all observed pathways. (A) Average FA. (B) Average MD. ns = not statistically significant ( $P > 0.05$ ), \* $P < 0.05$ , \*\* $P < 0.01$ , \*\*\* $P < 0.001$  (assessed using a two-tailed alpha). AD = Alzheimer’s disease dementia.

the uncinate fasciculus. In the Alzheimer’s disease dementia group, there were noticeable additional differences in temporal and prefrontal WM areas when compared with the HC group. Hence, again, these findings suggest an early regional vulnerability of posterior cholinergic WM in the Alzheimer’s disease continuum.

The same overall pattern of results could be observed when we repeated the voxel-wise analysis in the amyloid stratified subsample (Supplementary Figs 2 and 3). Despite the reduced statistical power, we again observed significant differences already in the SCD group, both in cingulum and external capsule pathways, which

became more prominent in the MCI and Alzheimer’s disease groups.

Contribution of the integrity of cholinergic pathways to cognitive performance

Figure 4 shows the degree of contribution of MD in cingulum and external capsule pathways, MD in remaining WM, WM hypointensities and NBM volume towards cognitive measures of memory and attention, as examined by RF analysis. Additional independent

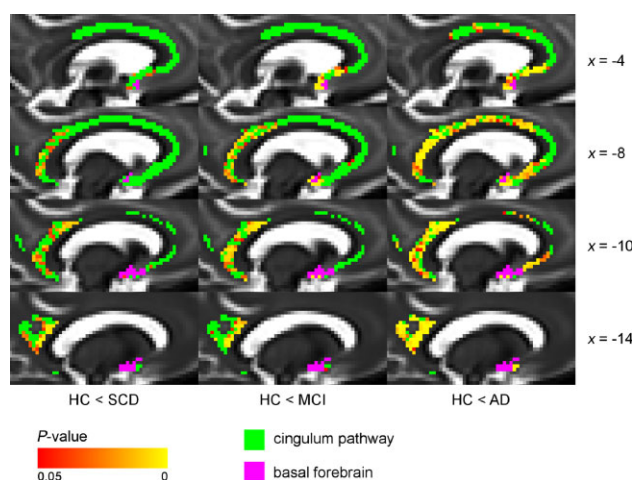


**Figure 2** Voxel-wise differences in MD between diagnostic groups and controls (cingulum pathway), controlling for age and sex. The cingulum pathway showed significantly higher MD values in the posterior/retrosplenial cingulate already in the SCD group compared with the HC group. Additional differences were present in the rostral and dorsal anterior cingulate in MCI and Alzheimer's disease dementia groups. Voxel-wise analyses of the diffusion data (MD values) were performed using non-parametric permutation testing. Identification of significant clusters in the data was performed using TFCE. Significance maps were corrected for multiple comparisons using a familywise error rate of  $P < 0.05$  (non-significant voxels are shown in green). BF mask (in purple) was inflated for illustrative purposes. AD = Alzheimer's disease dementia.

variables were age, sex and years of education. These analyses were conducted separately for the groups with normal cognition (HC and SCD) and the groups with impaired cognition (MCI and Alzheimer's disease dementia). Independent variables in each plot in Fig. 4 are presented in descending order of their importance score.

In the normal cognition groups (HC and SCD), sex, age and years of education were among the most important variables in the prediction of ADAS memory tests. MD in the external capsule pathway had a stronger importance in attention tests (Symbol digit modalities test, and Trail making test B). NBM volume and WM hypointensities received low importance scores in all the RF models. Scores from the Trail making test A failed to be predicted by the respective RF model.

In the impaired cognition groups (MCI and Alzheimer's disease dementia), NBM volume was among the most important predictors for ADAS word list learning and recall, Symbol digit modalities test and Trail making test B. MD in the external capsule pathway was important towards all ADAS memory tests and Trail making test A. MD in the cingulum pathway was a noticeable contributor only in the prediction of Trail making test A. WM hypointensities and MD in the remaining WM received low importance scores in all the RF models.

In summary, particularly the integrity of the external capsule pathway contributed to predict performance in attention tests in HC and SCD individuals. The contribution of cholinergic pathways (and NBM volume) to cognitive performance became stronger in the MCI and Alzheimer's disease dementia groups, both for memory and attention tests and also including the cingulum pathway.

### Integrity of cholinergic pathways discriminate the SCD group better than conventional volumetric measures (ROC analysis)

The ROC curves and their corresponding AUCs indicated how well each of the considered biomarkers can be used to distinguish

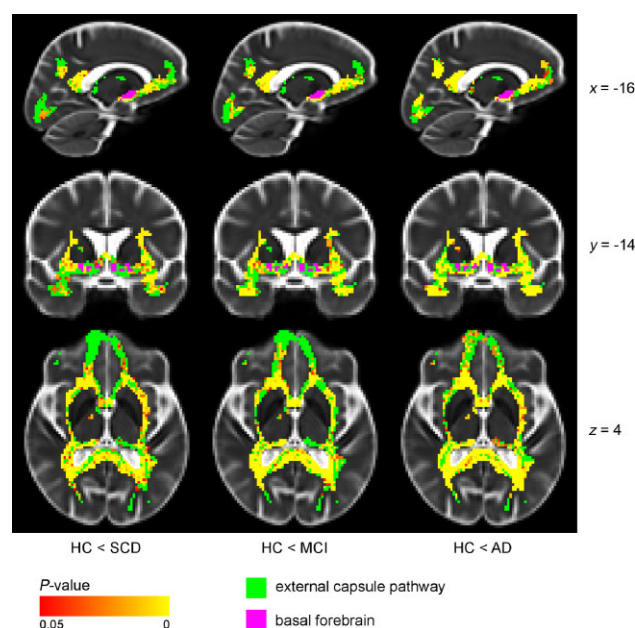


**Figure 3** Voxel-wise difference in MD between diagnostic groups and controls (external capsule pathway), controlling for age and sex. The external capsule pathway showed differences in the external capsule, posterior/retrosplenial cingulate and parts of the uncinate fasciculus in SCD and MCI compared with HC. Additional differences were present in temporal and prefrontal areas in the Alzheimer's disease dementia group. Voxel-wise analyses of the diffusion data (MD values) were performed using non-parametric permutation testing. Identification of significant clusters in the data was performed using TFCE. Significance maps were corrected for multiple comparisons using a familywise error rate of  $P < 0.05$  (statistically non-significant voxels are shown in green). BF mask (in purple) was inflated for illustrative purposes. AD = Alzheimer's disease dementia.

between a clinical group and the HC group. Please see Fig. 5 for P-values and Supplementary Table 5 for AUC values.

MD in the external capsule (ExCap) ( $AUC_{ExCap} = 0.736$ ) performed significantly better than all the other biomarkers in distinguishing SCD from HC. The second-best performing biomarker was MD in the cingulum (Cing) ( $AUC_{Cing} = 0.713$ ). AUCs of MD in the remaining WM (rem), NBM volume and hippocampus volume had the lowest discriminative performance and were not significantly different from each other:  $AUC_{MD\_rem} = 0.663$ ,  $AUC_{NBM\_vol} = 0.625$  and  $AUC_{hipp\_vol} = 0.660$ .

In the case of MCI, all biomarkers except for MD (rem. WM) reached statistically comparable high AUC values:  $AUC_{NBM\_vol} = 0.792$ ,  $AUC_{hipp\_vol} = 0.845$ ,  $AUC_{MD\_Cing} = 0.813$  and  $AUC_{MD\_ExCap} = 0.833$ . In contrast, MD (rem. WM) performed significantly poorer than all the other biomarkers ( $AUC_{MD\_rem} = 0.676$ ).

For the AD dementia group, hippocampus volume, NBM volume, and MD (ExCap) performed equally high:  $AUC_{hipp\_vol} = 0.936$ ,  $AUC_{NBM\_vol} = 0.936$  and  $AUC_{MD\_ExCap} = 0.901$ . P-values showed that MD (Cing) ( $AUC_{Cing} = 0.869$ ) showed slightly worse performance than hippocampus volume and MD (ExCap), and MD (rem. WM) had the worst value ( $AUC_{MD\_rem} = 0.745$ ).

In summary, the results of the ROC analysis were stage specific. Cholinergic WM pathways outperformed other biomarkers in the SCD group. Generally, all the considered biomarkers performed better with a more advanced clinical stage of the disease in the Alzheimer's disease continuum.

The findings were very similar in the amyloid stratified subsample (Supplementary Fig. 4 and Supplementary Table 4). In the



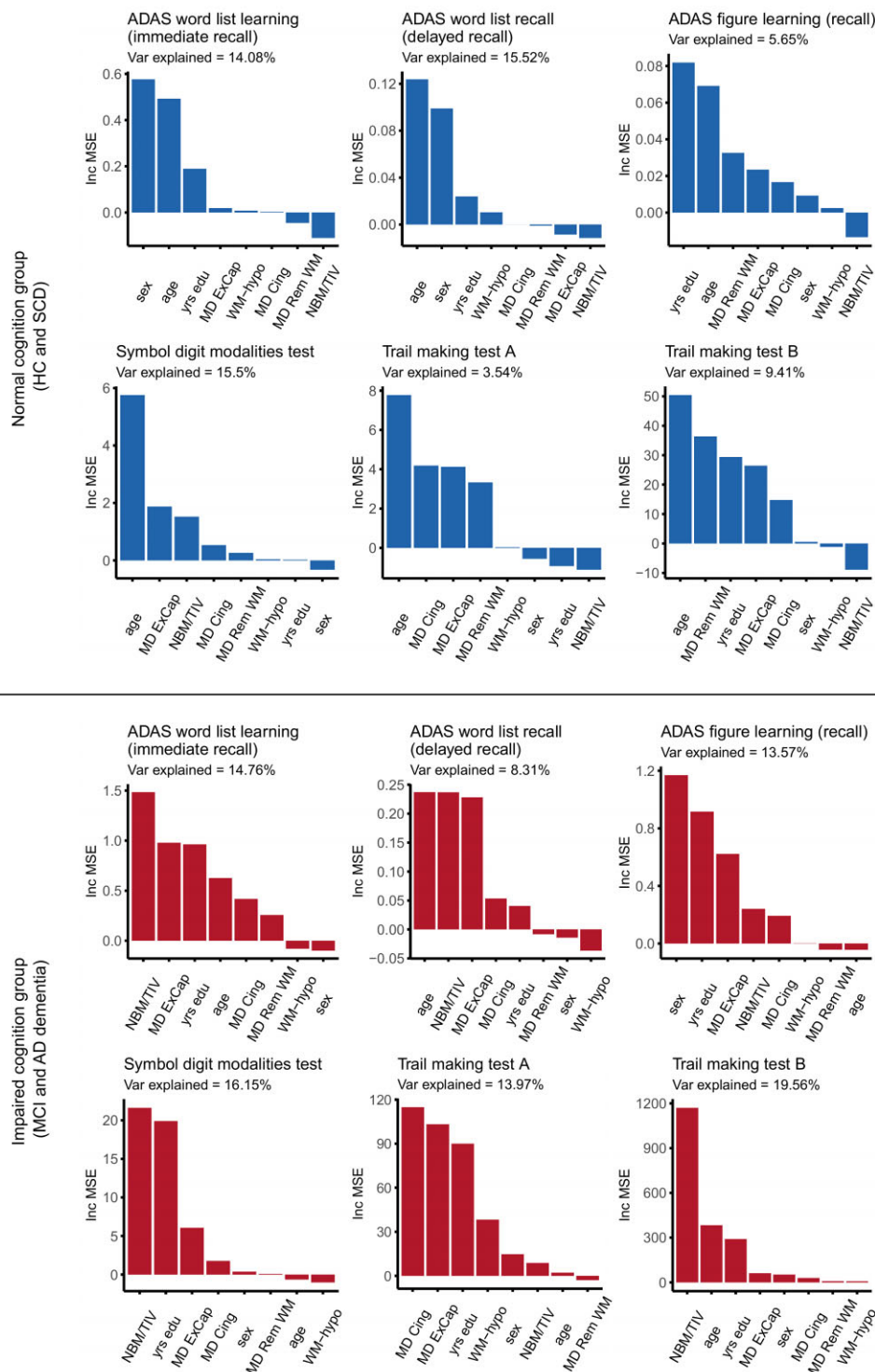


**Figure 4 RF models (increase in prediction error).** In the normal cognition groups (HC and SCD), MD in the external capsule pathway was important in predicting scores in attention tests, while NBM volume and WM hypointensities received low importance scores in all models. In the impaired cognition groups (MCI and Alzheimer's disease dementia), NBM volume and MD in external capsule and cingulum pathways were important in predicting scores in most memory and attention tests. ExCap = external capsule pathway; Cing = cingulum pathway; Rem WM = WM excluding cholinergic pathways; NBM/TIV = volume of NBM scaled by TIV; Var = variance; yrs = years. IncMSE = conditional variable importance computed by increase in the mean square error of prediction. This IncMSE is the result of a corresponding variable being permuted within a grid defined by the covariates that are associated to the variable of interest.

amyloid-positive SCD cases, the NBM volume performed worse than all the other biomarkers. In the amyloid-positive MCI cases, MD (Cing), MD (ExCap) and hippocampus volume were better

than NBM volume and MD (rem. WM). In the amyloid-positive AD dementia cases, all biomarkers performed better than MD (rem. WM).

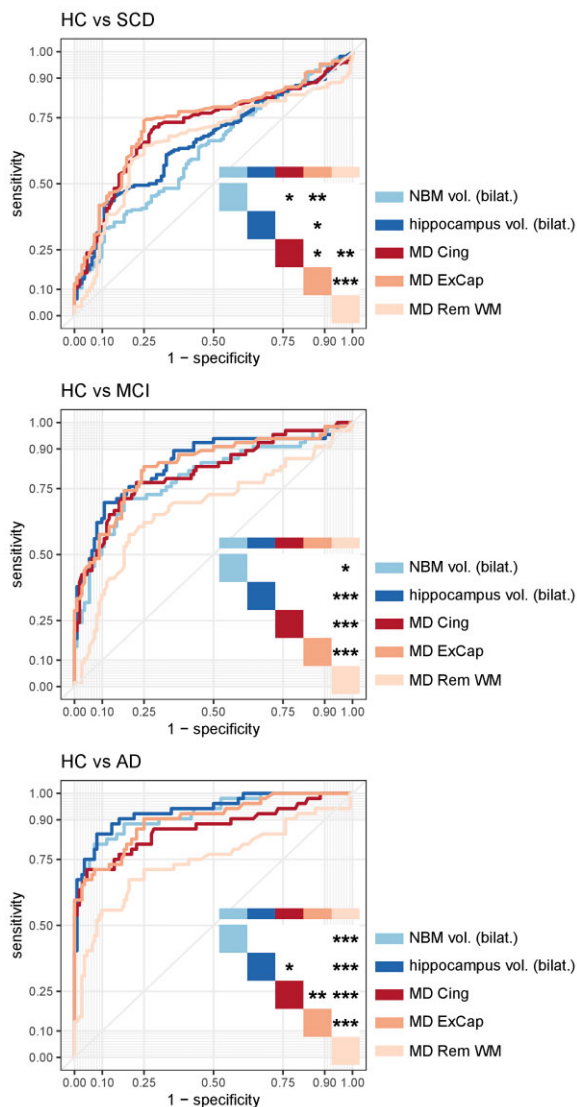


**Figure 5 ROC curves for diffusion and conventional MRI biomarkers.** The figures show that cholinergic WM pathways outperformed other MRI biomarkers in the SCD group, and that all considered biomarkers performed better with a more advanced clinical stage of the disease in the Alzheimer's disease continuum, in distinguishing between a clinical group and HC. \* $P < 0.05$ , \*\* $P < 0.01$ , \*\*\* $P < 0.001$  (assessed using a two-tailed alpha). AD = Alzheimer's disease dementia; ExCap = external capsule pathway; Cing = cingulum pathway; Rem WM = WM excluding cholinergic pathways; NBM vol. = volume of NBM scaled by TIV; hippocampus vol. = volume of hippocampus scaled by TIV.

## Discussion

We investigated DTI-based integrity of the human cholinergic system along the Alzheimer's disease continuum, including SCD individuals as a group reflecting the preclinical stage of Alzheimer's disease (particularly amyloid-positive SCD individuals). The study focused on the integrity of the cholinergic WM pathways, including differences between clinical stages, their predictive power compared to conventional volumetric MRI biomarkers, and their association to cognitive performance. We found reduced integrity of the cholinergic pathways in all the stages of the Alzheimer's disease continuum (SCD, MCI and Alzheimer's disease dementia). The spatial distribution of these differences followed a posterior–anterior

pattern. Differences in the SCD stage involved posterior cholinergic WM and, at more advanced stages, we also found differences in anterior frontal WM. All considered biomarkers (conventional volumetric and novel measures of WM integrity) showed higher predictive power at more advanced stages within the Alzheimer's disease continuum. However, measures of the integrity of the cholinergic pathways were more informative in distinguishing SCD from HC than all other biomarkers. The multivariate models showed that the integrity of the cholinergic pathways and NBM volume, but not the integrity of the rest of WM, strongly contributed to performance in attention and memory in cognitively impaired individuals (MCI and Alzheimer's disease dementia).

In the whole sample, we found that the integrity of the cholinergic WM pathways was reduced in all stages of the Alzheimer's disease continuum. The findings for the MCI and Alzheimer's disease dementia groups thus agree with a recent study that showed that NBM degeneration is accompanied by alterations of cholinergic WM pathways in MCI and Alzheimer's disease dementia.<sup>14</sup> Additionally, a recent post-mortem study based on post-mortem MRI and histopathology reported no significant differences between Alzheimer's disease and HC in cholinergic WM pathways, but demonstrated that decreased cholinergic cell density in NBM was associated with reduced integrity of cholinergic WM pathways towards the temporal lobe.<sup>51</sup> Our current study extends these previous studies by showing that the integrity of cholinergic pathways is already altered at the stage of SCD.

We did not observe any statistically significant differences in CSF biomarkers between the SCD and HC groups. These results are in line with previous studies that showed no significant differences in CSF biomarkers in SCD compared to HC.<sup>52–55</sup> There are, however, some reports about significant differences in CSF biomarkers between SCD and HC groups.<sup>56</sup> These differences have also been observed in CSF and PET AD biomarkers in SCD individuals who progressed to MCI or dementia.<sup>57,58</sup> The observed lack of statistical differences in our study and by others could mean that degeneration of the cholinergic system may precede measurable changes in conventional biomarkers for Alzheimer's disease pathology ( $A\beta$  and tau biomarkers). A similar conclusion has been made by a study of BF volume.<sup>9</sup> Alternatively, perhaps more sensitive CSF biomarkers such as N-224 could detect Alzheimer's disease pathology in the absence of statistical differences for  $A\beta_{42}/A\beta_{40}$  ratio and p-tau181 CSF biomarkers.<sup>56,59</sup>

The reduced integrity of the cholinergic pathways in all stages of the Alzheimer's disease continuum was replicated in the amyloid stratified subsample, thus supporting our findings both in clinically and biologically defined study groups. In addition, the integrity of the remaining WM was reduced in all stages of the continuum, in the whole sample. This global WM degeneration has also been reported by others.<sup>60</sup> However, this reduction of integrity of remaining WM could not be clearly observed in the amyloid stratified subsample. Although this could be explained by the small sample size, the integrity of both cholinergic pathways remained significantly different between clinical groups and HC in the amyloid stratified subsample, hence, with the same sample size. This could possibly mean that while the remaining WM deteriorates and its changes in integrity provide information about the global degeneration, the considered cholinergic pathways and their integrity are particularly sensitive to an Alzheimer's pathologic change ( $A\beta$  positivity). This hypothesis could be further supported by our statistically significant correlation between CSF  $A\beta$  levels and integrity of cingulum and external capsule pathways. In addition, we also showed a statistically significant correlation between CSF tau

biomarkers and integrity of cingulum and external capsule pathways, supporting the association between cholinergic WM and Alzheimer's disease-related pathology. Although there are no studies investigating *in vivo* cholinergic projections in Alzheimer's disease other than the recent study by Schumacher *et al.*,<sup>14</sup> studies focusing on NBM volume similarly reported that NBM volume is more closely associated with Alzheimer's disease-related pathology than other GM areas.<sup>9,61</sup> This finding is also supported by our ROC analysis, in which the integrity of remaining WM performed consistently poorer in all cases.

Another finding this study provides is the spatial distribution of differences in WM integrity of the cholinergic pathways, along the Alzheimer's disease continuum. We demonstrated that the SCD group already showed a clear pattern of reduced integrity in the retrosplenial and posterior cingulate cortex, as well as in the external capsule. These regions were previously identified as the ones with the earliest neuronal and metabolic changes and reduced connectivity, emerging as a vulnerable Alzheimer's disease-associated epicentre.<sup>62</sup> Also, these regions have been associated with early accumulation of amyloid in PET studies.<sup>63</sup> Differences in the MCI group included the same areas as in the SCD group and, additionally, involved the rostral anterior cingulate. In Alzheimer's disease dementia, WM integrity alterations extended to the dorsal anterior cingulate and temporal and prefrontal areas. These areas are usually associated with increased neuronal loss in MCI and Alzheimer's disease dementia,<sup>64</sup> but here we show involvement of the cholinergic WM. Despite the cross-sectional nature of our analyses, the replication of regional damage as the disease progresses, as well as the stepwise addition of cholinergic WM areas following a posterior–anterior pattern of degeneration is a robust finding. If replicated in longitudinal designs, these findings could help understanding the progression of cholinergic system changes *in vivo*, along the development of Alzheimer's disease.

Finally, RF analysis showed a substantially different set of important predictors of cognitive scores in cognitively unimpaired and impaired groups. In the analysis of HC and SCD groups combined, it was mainly age, sex and years of education that counted towards the cognitive performance. On top of that, the integrity of the external capsule pathway played a moderately important role in tests of attention. The external capsule pathway projects to cortices involved in attention such as regions located in frontal lobe and posterior cortex. On the other hand, in the analysis involving cognitively impaired groups (MCI and Alzheimer's disease dementia), integrity in the external capsule and cingulum pathways was important towards most of the tests of memory and attention. In addition to frontal and posterior cortical areas, the external capsule pathway also projects to cortices related to memory such as medial temporal structures. The cingulum pathway also projects to cortices related to memory such as hippocampal structures and posterior cingulate cortex. These findings reflect the role of cholinergic system in cognitive process of effortful attention and memory. Integrity in the remaining WM was not important. Similar results have recently been reported in studies conducted in healthy ageing<sup>27</sup> and in Alzheimer's disease and dementia with Lewy bodies.<sup>14,51</sup> In our cognitively unimpaired groups (HC and SCD), we could practically replicate the results in Nemy *et al.*<sup>27</sup> that were based on independent data. First, we observed that age and sex were important variables towards the prediction of most of the cognitive tests. Second, the integrity of cholinergic pathways received considerably high importance score only towards tests involving effortful attention. The difference in average age of 15 years between our current cohort and the participants in Nemy *et al.*<sup>27</sup>

suggests that these findings may be generalizable across age groups. In addition, in the current study we observed that NBM volume was important towards performance in memory and attention tests in the MCI and Alzheimer's disease dementia groups. This is in line with other studies investigating Alzheimer's disease<sup>65</sup> and Parkinson's disease,<sup>66</sup> which found that NBM volume is an important predictor of disease progression. Altogether, these findings suggest that the cholinergic system may deteriorate earlier in the WM, and NBM volume would follow in more advanced stages of the disease. In keeping with the posterior–anterior pattern of WM cholinergic disruption, this observation might suggest that NBM starts deteriorating when enough cholinergic WM damage has occurred. This dying-back pattern of degeneration known as 'Wallerian-like degeneration' has been demonstrated in Alzheimer's disease in several experimental and pathological studies.<sup>11,67</sup> All in all, these results illustrate the early involvement of cholinergic pathways in the Alzheimer's disease continuum and add additional evidence that the used methodology using DTI tracking is a promising and emerging potential biomarker of microstructural changes within earliest stages of Alzheimer's disease.

All the findings discussed here are further underlined by the results of our ROC analysis. First, all considered biomarkers, both conventional volumetric and novel measures of WM integrity, showed higher predictive importance with the progression of the disease. This finding validates the conventional volumetric biomarkers but also suggests that the proposed measures of WM integrity are sensitive to neurodegeneration changes along the Alzheimer's disease continuum. Consistent low predictive power of remaining WM integrity in ROC analysis points out that the measures of the cholinergic system pathways are not only sensitive but also specific. Second, the ROC data showed significantly better predictive power of integrity of cholinergic WM pathways than the conventional volumetric measures in the SCD group. This might suggest that the proposed cholinergic biomarkers are more suitable for detecting very early changes in the disease. Third, whereas in the whole sample the predictive power of the NBM volume appeared approximately on the same level as the integrity of at least one of the cholinergic WM pathways, in the amyloid-positive subsample the NBM volume performed significantly worse than both cholinergic WM pathways in distinguishing SCD and MCI from HC. This further supports the hypothesis that alterations of cholinergic WM projections occur earlier than neurodegeneration in NBM, in the context of an Alzheimer's pathologic change (A $\beta$  positivity).

This study has some limitations. We primarily aimed to investigate cross-sectional differences along the Alzheimer's disease continuum and interpretations about cholinergic WM pathways and clinical progression were based on different groups. Whereas this approach serves as a preliminary demonstration of early differences in cholinergic WM pathways in the SCD group, that extends to other WM areas in the MCI and Alzheimer's disease dementia groups, it will be important to expand our current approach to include longitudinal analyses in the future. Longitudinal analyses will be needed to confirm our preliminary interpretation of cholinergic alterations preceding Alzheimer's disease pathology (positivity both in A $\beta$  and tau biomarkers). Next, CSF biomarkers were not available for all subjects in the cohort. Although the CSF biomarker subsample was large enough to allow for replication of the main results, the analysis would benefit from having an even larger CSF sample. Our comparison of participants with and without CSF data available did not show any difference in terms of key demographic variables and MMSE scores, suggesting a low risk for selection bias with regards the subsample with CSF data available.



Furthermore, even with standardized MRI acquisition protocols and careful image quality control, we cannot completely exclude that inter-scanner variance may have influenced some of our results.<sup>68</sup> However, since the focus of this study mostly involved comparison of within-subject measures (i.e. conventional volumetric versus cholinergic WM integrity biomarkers), our main conclusions should not be affected by inter-scanner variance. We also provide the breakdown of study participants by scanner in [Supplementary Table 7](#), for the reader's interest. Last, voxel-wise analysis showed significant differences in MD in posterior parts of the cholinergic pathways between SCD and HC. However, when using an average measure of MD in the entire cholinergic pathways, we did not observe a pronounced contribution of the cholinergic pathways to cognition in the RF models. Future studies could explore the contribution of more regional measures of MD to cognitive performance in SCD individuals.

In conclusion, we modelled *in vivo* cholinergic WM pathways and investigated their integrity along the stages of the Alzheimer's disease continuum, and in relation to cognitive performance. We showed that the integrity of the cholinergic WM pathways is associated to Alzheimer's disease-related pathology, and it reveals alterations as early as the stage of SCD. The cholinergic WM pathways differentiated between SCD and HC groups better than the integrity of non-cholinergic WM and conventional measures of hippocampal and NBM volumes. These findings suggest that the integrity of WM cholinergic pathways is a sensitive and specific biomarker of early neurodegeneration in individuals with an Alzheimer's pathologic change (A $\beta$  positivity).

## Funding

This study was supported by the Swedish Research Council (2020-02014); the regional agreement on medical training and clinical research (ALF) between Stockholm County Council and Karolinska Institutet; Center for Innovative Medicine (CIMED); the Swedish Alzheimer Foundation; the Swedish Brain Foundation; Neuro Fonden, the Czech Alzheimer Foundation; and Demensfonden. Research by M.N., O.S. and L.V. was partially supported by institutional resources of Czech Technical University in Prague. The work was further supported by a grant to S.J.T. within the CureDem funding of the Bundesministerium für Bildung und Forschung (BMBF), grant number 01KX2130. The funding sources did not have any involvement in the study design; collection, analysis and interpretation of data; writing of the report and the decision to submit the article for publication.

## Competing interests

S.J.T. participated in scientific advisory boards of Roche Pharma AG, Biogen, GRIFOLS, Eisai and MSD and received lecture fees from Roche and MSD. The other authors report no competing interests.

## Supplementary material

[Supplementary material](#) is available at *Brain* online.

## References

- Buchhave P, Minthon L, Zetterberg H, Wallin ÅK, Blennow K, Hansson O. Cerebrospinal fluid levels of  $\beta$ -amyloid 1–42, but not of tau, are fully changed already 5 to 10 years before the onset of Alzheimer dementia. *Arch Gen Psychiatry*. 2012;69:98–106.
- Villemagne VL, Burnham S, Bourgeat P, et al. Amyloid  $\beta$  deposition, neurodegeneration, and cognitive decline in sporadic Alzheimer's disease: A prospective cohort study. *Lancet Neurol*. 2013;12:357–367.
- Albert M, Zhu Y, Moghekar A, et al. Predicting progression from normal cognition to mild cognitive impairment for individuals at 5 years. *Brain*. 2018;141:877–887.
- Sperling RA, Aisen PS, Beckett LA, et al. Toward defining the pre-clinical stages of Alzheimer's disease: Recommendations from the National Institute on Aging-Alzheimer's Association workgroups on diagnostic guidelines for Alzheimer's disease. *Alzheimer's Dement*. 2011;7:280–292.
- Dubois B, Hampel H, Feldman HH, et al. Preclinical Alzheimer's disease: Definition, natural history, and diagnostic criteria. *Alzheimer's Dement*. 2016;12:292–323.
- Jack CR, Bennett DA, Blennow K, et al. NIA-AA research framework: Toward a biological definition of Alzheimer's disease. *Alzheimer's Dement*. 2018;14:535–562.
- Fu H, Hardy J, Duff KE. Selective vulnerability in neurodegenerative diseases. *Nat Neurosci*. 2018;21:1350–1358.
- Brueggen K, Dyrba M, Barkhof F, et al. Basal forebrain and hippocampus as predictors of conversion to Alzheimer's disease in patients with mild cognitive impairment—A multicenter DTI and volumetry study. *J Alzheimer's Dis*. 2015;48:197–204.
- Schmitz TW, Nathan Spreng R, Alzheimer's Disease Neuroimaging Initiative. Basal forebrain degeneration precedes and predicts the cortical spread of Alzheimer's pathology. *Nat Commun*. 2016;7:13249.
- Bartus RT, Dean RL, Beer B, Lippa AS. The cholinergic hypothesis of geriatric memory dysfunction. *Science*. 1982;217:408–414.
- Kanaan NM, Pigino GF, Brady ST, Lazarov O, Binder LI, Morfini GA. Axonal degeneration in Alzheimer's disease: When signaling abnormalities meet the axonal transport system. *Exp Neurol*. 2013;246:44–53.
- Li X, Li TQ, Andreasen N, Wiberg MK, Westman E, Wahlund LO. The association between biomarkers in cerebrospinal fluid and structural changes in the brain in patients with Alzheimer's disease. *J Intern Med*. 2014;275:418–427.
- Li X, Westman E, Ståhlbom AK, et al. White matter changes in familial Alzheimer's disease. *J Intern Med*. 2015;278:211–218.
- Schumacher J, Ray NJ, Hamilton CA, et al. Cholinergic white matter pathways in dementia with Lewy bodies and Alzheimer's disease. *Brain*. 2022;145(5):1773–1784.
- Ballinger EC, Ananth M, Talmage DA, Role LW. Basal forebrain cholinergic circuits and signaling in cognition and cognitive decline. *Neuron*. 2016;91:1199–1218.
- Jessen F, Spottke A, Boecker H, et al. Design and first baseline data of the DZNE multicenter observational study on pre-dementia Alzheimer's disease (DELCODE). *Alzheimer's Res Ther*. 2018;10:21.
- Folstein MF, Folstein SE, McHugh PR. "Mini-mental state": A practical method for grading the cognitive state of patients for the clinician. *J Psychiatr Res*. 1975;12:189–198.
- Yesavage JA, Sheikh JI. Geriatric Depression Scale (GDS). *Clin Gerontol*. 1986;5:165–173.
- Jessen F, Amariglio RE, Van Boxtel M, et al. A conceptual framework for research on subjective cognitive decline in preclinical Alzheimer's disease. *Alzheimer's Dement*. 2014;10:844–852.
- Albert MS, DeKosky ST, Dickson D, et al. The diagnosis of mild cognitive impairment due to Alzheimer's disease: Recommendations from the National Institute on Aging-Alzheimer's

- Association workgroups on diagnostic guidelines for Alzheimer's disease. *Alzheimer's Dement.* 2011;7:270-279.
21. McKhann GM, Knopman DS, Chertkow H, et al. The diagnosis of dementia due to Alzheimer's disease: Recommendations from the National Institute on Aging-Alzheimer's Association workgroups on diagnostic guidelines for Alzheimer's disease. *Alzheimer's Dement.* 2011;7:263-269.
  22. Mohs RC, Knopman D, Petersen RC, et al. Development of cognitive instruments for use in clinical trials of antidementia drugs: Additions to the Alzheimer's disease assessment scale that broaden its scope. *Alzheimer Dis Assoc Disord.* 1997;11:13-21.
  23. Smith A. *Symbol digit modality test (SDMT): Manual (revised)*. Western Psychological Services; 1982.
  24. Reitan RM. Validity of the trail making test as an indicator of organic brain damage. *Percept Mot Skills.* 1958;8:271-276.
  25. Janelidze S, Zetterberg H, Mattsson N, et al. CSF A $\beta$ 42/A $\beta$ 40 and A $\beta$ 42/A $\beta$ 38 ratios: Better diagnostic markers of Alzheimer disease. *Ann Clin Transl Neurol.* 2016;3:154-165.
  26. Jezzard P, Balaban RS. Correction for geometric distortion in echo planar images from B0 field variations. *Magn Reson Med.* 1995;34:65-73.
  27. Nemy M, Cedres N, Grothe MJ, et al. Cholinergic white matter pathways make a stronger contribution to attention and memory in normal aging than cerebrovascular health and nucleus basalis of Meynert. *Neuroimage.* 2020;211:116607.
  28. Jenkinson M, Beckmann CF, Behrens TEJ, Woolrich MW, Smith SM. FSL. *Neuroimage.* 2012;62:782-790.
  29. Smith SM. Fast robust automated brain extraction. *Hum Brain Mapp.* 2002;17:143-155.
  30. Reber PJ, Wong EC, Buxton RB, Frank LR. Correction of off resonance-related distortion in echo-planar imaging using EPI-based field maps. *Magn Reson Med.* 1998;39:328-330.
  31. Andersson JLR, Sotiropoulos SN. An integrated approach to correction for off-resonance effects and subject movement in diffusion MR imaging. *Neuroimage.* 2016;125:1063-1078.
  32. Behrens TEJ, Berg HJ, Jbabdi S, Rushworth MFS, Woolrich MW. Probabilistic diffusion tractography with multiple fibre orientations: What can we gain? *Neuroimage.* 2007;34:144-155.
  33. Hernández M, Guerrero GD, Cecilia JM, et al. Accelerating fibre orientation estimation from diffusion weighted magnetic resonance imaging using GPUs. *PLoS ONE.* 2013;8:e61892.
  34. Selden NR, Gitelman DR, Salamon-Murayama N, Parrish TB, Mesulam MM. Trajectories of cholinergic pathways within the cerebral hemispheres of the human brain. *Brain.* 1998;121:2249-2257.
  35. Kilimann I, Grothe M, Heinsen H, et al. Subregional basal forebrain atrophy in Alzheimer's disease: A multicenter study. *J Alzheimer's Dis.* 2014;40:687-700.
  36. Mori S, Wakana S, Van Zijl PC, Nagae-Poetscher L. *MRI atlas of human white matter*. Elsevier; 2005.
  37. Behrens TEJ, Woolrich MW, Jenkinson M, et al. Characterization and propagation of uncertainty in diffusion-weighted MR imaging. *Magn Reson Med.* 2003;50:1077-1088.
  38. Zhang Y, Brady M, Smith S. Segmentation of brain MR images through a hidden Markov random field model and the expectation-maximization algorithm. *IEEE Trans Med Imaging.* 2001;20:45-57.
  39. Buckner RL, Head D, Parker J, et al. A unified approach for morphometric and functional data analysis in young, old, and demented adults using automated atlas-based head size normalization: Reliability and validation against manual measurement of total intracranial volume. *Neuroimage.* 2004;23:724-738.
  40. Kim HJ, Moon WJ, Han SH. Differential cholinergic pathway involvement in Alzheimer's disease and subcortical ischemic vascular dementia. *J Alzheimer's Dis.* 2013;35:129-136.
  41. Cedres N, Ferreira D, Machado A, et al. Predicting Fazekas scores from automatic segmentations of white matter signal abnormalities. *Aging (Albany NY).* 2020;12:894-901.
  42. Leritz EC, Shepel J, Williams VJ, et al. Associations between T1 white matter lesion volume and regional white matter microstructure in aging. *Hum Brain Mapp.* 2014;35:1085-1100.
  43. Fischl B, Salat DH, Busa E, et al. Whole brain segmentation: Automated labeling of neuroanatomical structures in the human brain. *Neuron.* 2002;33:341-355.
  44. Winkler AM, Ridgway GR, Webster MA, Smith SM, Nichols TE. Permutation inference for the general linear model. *Neuroimage.* 2014;92:381-397.
  45. Cedres N, Ferreira D, Nemy M, et al. Association of cerebrovascular and Alzheimer disease biomarkers with cholinergic white matter degeneration in cognitively unimpaired individuals. *Neurology.* 2022;99(15):e1619-e1629.
  46. Breiman L. Random forests. *Mach Learn.* 2001;45:5-32.
  47. Breiman L. Bagging predictions. *Mach Learn.* 1996;24:123-140.
  48. Lebedev AV, Westman E, Van Westen GJP, et al. Random forest ensembles for detection and prediction of Alzheimer's disease with a good between-cohort robustness. *Neuroimage Clin.* 2014;6:115-125.
  49. Strobl C, Boulesteix AL, Zeileis A, Hothorn T. Bias in random forest variable importance measures: Illustrations, sources and a solution. *BMC Bioinf.* 2007;8:25.
  50. Robin X, Turck N, Hainard A, et al. pROC: An open-source package for R and S+ to analyze and compare ROC curves. *BMC Bioinf.* 2011;12:77.
  51. Lin C-P, Frigerio I, Boon BDC, et al. Structural (dys)connectivity associates with cholinergic cell density in Alzheimer's disease. *Brain.* 2022;145:2869-2881.
  52. Wolfgruber S, Kleineidam L, Guski J, et al. Minor neuropsychological deficits in patients with subjective cognitive decline. *Neurology.* 2020;95:e1134-e1143.
  53. Rami L, Fortea J, Bosch B, et al. Cerebrospinal fluid biomarkers and memory present distinct associations along the continuum from healthy subjects to AD patients. *J Alzheimer's Dis.* 2011;23:319-326.
  54. Visser PJ, Verhey F, Knol DL, et al. Prevalence and prognostic value of CSF markers of Alzheimer's disease pathology in patients with subjective cognitive impairment or mild cognitive impairment in the DESCRIPA study: A prospective cohort study. *Lancet Neurol.* 2009;8:619-627.
  55. Antonell A, Fortea J, Rami L, et al. Different profiles of Alzheimer's disease cerebrospinal fluid biomarkers in controls and subjects with subjective memory complaints. *J Neural Transm.* 2011;118:259-262.
  56. Sánchez-Benavides G, Suárez-Calvet M, Milà-Alomà M, et al. Amyloid- $\beta$  positive individuals with subjective cognitive decline present increased CSF neurofilament light levels that relate to lower hippocampal volume. *Neurobiol Aging.* 2021;104:24-31.
  57. Ferreira D, Falahati F, Linden C, et al. A "disease severity index" to identify individuals with subjective memory decline who will progress to mild cognitive impairment or dementia. *Sci Rep.* 2017;7:44368.
  58. Ebenau JL, Pelkmans W, Verberk IMW, et al. Association of CSF, plasma, and imaging markers of neurodegeneration with clinical progression in people with subjective cognitive decline. *Neurology.* 2022;98:E1315-E1326.
  59. Cicognola C, Hansson O, Scheltens P, et al. Cerebrospinal fluid N-224 tau helps discriminate Alzheimer's disease from subjective cognitive decline and other dementias. *Alzheimer's Res Ther.* 2021;13:38.

60. Sun X, Salat D, Upchurch K, Deason R, Kowall N, Budson A. Destruction of white matter integrity in patients with mild cognitive impairment and Alzheimer disease. *J Investig Med*. 2014; 62:927-933.
61. Teipel S, Heinsen H, Amaro E, et al. Cholinergic basal forebrain atrophy predicts amyloid burden in Alzheimer's disease. *Neurobiol Aging*. 2014;35:482-491.
62. Lee PL, Chou KH, Chung CP, et al. Posterior cingulate cortex network predicts Alzheimer's disease progression. *Front Aging Neurosci*. 2020;12:466.
63. Palmqvist S, Schöll M, Strandberg O, et al. Earliest accumulation of  $\beta$ -amyloid occurs within the default-mode network and concurrently affects brain connectivity. *Nat Commun*. 2017;8:1-13.
64. Coughlan G, Laczó J, Hort J, Miniñane AM, Hornberger M. Spatial navigation deficits—overlooked cognitive marker for preclinical Alzheimer disease? *Nat Rev Neurol*. 2018;14:496-506.
65. Fernández-Cabello S, Kronbichler M, van Dijk KRA, Goodman JA, Nathan Spreng R, Schmitz TW. Basal forebrain volume reliably predicts the cortical spread of Alzheimer's degeneration. *Brain*. 2020;143:993-1009.
66. Schulz J, Pagano G, Fernández Bonfante JA, Wilson H, Politis M. Nucleus basalis of Meynert degeneration precedes and predicts cognitive impairment in Parkinson's disease. *Brain*. 2018;141: 1501-1516.
67. Nishioka C, Liang HF, Barsamian B, Sun SW. Amyloid-beta induced retrograde axonal degeneration in a mouse tauopathy model. *Neuroimage*. 2019;189:180-191.
68. Teipel SJ, Kuper-Smith JO, Bartels C, et al. Multicenter tract-based analysis of microstructural lesions within the Alzheimer's disease Spectrum: Association with amyloid pathology and diagnostic usefulness. *J Alzheimers Dis*. 2019;72: 455-465.